Mon. Not. R. Astron. Soc. **000**, 1–?? (2008) Printed 8 May 2008 (MN LaTeX style file v2.2)

Galactic clusters with associated Cepheid variables. VII. Berkeley 58 and CG Cassiopeiae

D. G. Turner[1,9,10,11]⋆, D. Forbes[2,9], D. English[2,10], P. J. T. Leonard[3], J. N. Scrimger[4], A. W. Wehlau[5], R. L. Phelps[6,9], L. N. Berdnikov[7,11] and E. N. Pastukhova[8]

[1] *Department of Astronomy and Physics, Saint Mary's University, Halifax, NS B3H 3C3, Canada*
[2] *Department of Physics, Sir Wilfred Grenfell College, Memorial University of Newfoundland, Corner Brook, NF A2H 6P9, Canada*
[3] *ADNET Systems, Inc., 7515 Mission Dr., Suite A1C1, Lanham, Maryland 20706, U.S.A.*
[4] *Faculty of Computer Science, Dalhousie University, Halifax, NS B3H 1W5, Canada*
[5] *Department of Physics and Astronomy, The University of Western Ontario, London, ON N6A 3K7, Canada*
[6] *Office of Integrative Activities, National Science Foundation, Division of Astronomical Sciences, 4201 Wilson Blvd., Arlington, Virginia 22230, U.S.A.*
[7] *Sternberg Astronomical Institute, 13 Universitetskij prosp., Moscow 119992, Russia*
[8] *Institute of Astronomy, Russian Academy of Sciences, 48 Pyatnitskaya ul., Moscow 109017, Russia*
[9] *Visiting Astronomer, Kitt Peak National Observatory, National Optical Astronomy Observatories, which is operated by the Association of Universities for Research in Astronomy, Inc. (AURA) under co-operative agreement with the National Science Foundation*
[10] *Visiting Astronomer, Dominion Astrophysical Observatory, Herzberg Institute of Astrophysics, National Research Council of Canada*
[11] *Visiting Astronomer, Harvard College Observatory Photographic Plate Stacks*

Accepted 2008 May 1. Received 2008 May 1; in original form 2008 March 31

ABSTRACT

Photoelectric, photographic, and CCD UBV photometry, spectroscopic observations, and star counts are presented for the open cluster Berkeley 58 to examine a possible association with the $4^{\rm d}.37$ Cepheid CG Cas. The cluster is difficult to separate from the early-type stars belonging to the Perseus spiral arm, in which it is located, but has reasonably well-defined parameters: an evolutionary age of $\sim 10^8$ years, a mean reddening of $\mathrm{E}_{B-V}(\mathrm{B0}) = 0.70 \pm 0.03$ s.e., and a distance of 3.03 ± 0.17 kpc ($V_0 - M_V = 12.40 \pm 0.12$ s.d.). CG Cas is a likely cluster coronal member on the basis of radial velocity, and its period increase of $+0.170 \pm 0.014$ s yr^{-1} and large light amplitude describe a Cepheid in the third crossing of the instability strip lying slightly blueward of strip centre. Its inferred reddening and luminosity are $\mathrm{E}_{B-V} = 0.64 \pm 0.02$ s.e. and $\langle M_V \rangle = -3.06 \pm 0.12$. A possible K supergiant may also be a cluster member.

Key words: stars: variables: Cepheids—stars: evolution—Galaxy: open clusters and associations: individual: Berkeley 58.

1 INTRODUCTION

After the rediscovery in the early 1950s of spatial coincidences between Cepheids and open clusters by Irwin (1955, 1958), Eggen (see Sandage 1958), and Kholopov (1956), a number of searches for additional coincidences were made by Kraft (1957), van den Bergh (1957), and Tifft (1959), among others. Tifft's search resulted in the discovery of a near spatial coincidence between the $4^{\rm d}.37$ Cepheid CG Cassiopeiae and an anonymous open cluster, subsequently catalogued as Berkeley 58 (Setteducati & Weaver 1962), which lies less than one cluster diameter to the west. The field is coincident with a portion of the Perseus spiral arm that is relatively rich in open clusters, and the cluster NGC 7790 with its three Cepheid members lies in close proximity. The possibility that CG Cas might be an outlying member of NGC 7790 was raised at one time by Efremov (1964a,b), and found some support in a star count analysis by Kovalenko (1968). More detailed star counts in the field (Turner 1985) indicate otherwise, as do the available proper motion data (Frolov 1974, 1977). The Cepheid does lie in the corona of Berkeley 58 (Turner 1985), although Frolov has argued that it is not a probable cluster member.

Given a probable distance of 3 kpc to both CG Cas and Berkeley 58 (e.g., Frolov 1979; Phelps & Janes 1994), it is not clear that existing proper motion data are precise enough to provide conclusive evidence pertaining to the

⋆ Email: turner@ap.smu.ca

cluster membership of CG Cas. The present study was therefore initiated in order to examine the case in more detail. As demonstrated here, there is strong evidence that CG Cas is a likely member of Berkeley 58 and that it can serve as a calibrator for the Cepheid period-luminosity (PL) relation.

2 OBSERVATIONAL DATA

A variety of observations were obtained for the present investigation. Table 1 presents photoelectric *UBV* photometry for bright members of Berkeley 58, obtained during observing runs at Kitt Peak National Observatory in 1981 September, 1982 August, and 1984 August. The data, acquired using 1P21 photomultipliers and standard *UBV* filter sets used in conjunction with pulse-counting photometers on the No. 4–0.4-m, No. 2–0.9-m, and 1.3-m telescopes at Kitt Peak, have associated uncertainties typical of our previous investigations of Cepheid clusters (Turner et al. 1992; Turner 1992; Turner et al. 1994), namely standard internal errors for a single observation of ± 0.01 in V and B–V, and ± 0.02 in U–B, for stars brighter than $V = 13$. The estimated external errors for all but the faintest stars are similar in magnitude. The stars are identified by their numbering in Fig. 1, as well as by their 2000 co-ordinates in the 2MASS survey (Cutri et al. 2003); the number of individual observations for each star is given in column 7 of Table 1.

Star 6 is the eclipsing system V654 Cas, for which Berdnikov (1993) cites photoelectric values of V and B–V outside of eclipse that are close to the values given here. Star 30 is a close optical double with components of nearly identical brightness. The photoelectric values apply to the combined light from both stars, whereas CCD observations provide uncontaminated data for the southwestern star of the pair, as established by its CCD magnitude being 0.75 mag. fainter. By contrast, the CCD V magnitude for star 35 is 0.21 mag. brighter, which suggests possible variability in the object. Individual photoelectric observations for CG Cas are presented in Table 2.

Photographic *UBV* photometry was also obtained for stars in the nuclear and coronal regions of Berkeley 58 from photographic plates of the cluster field obtained in 1984 September using the 1.2-m Elginfield telescope of the University of Western Ontario. The star images were measured using the iris diaphragm photometer at Saint Mary's University, and were reduced to the *UBV* system and calibrated with reference to the photoelectric standards identified in Table 1 using the techniques discussed by Turner & Welch (1989). The resulting data are presented in Table 3 (Appendix) in similar format to the data of Table 1, and the stars are identified by their 2000 co-ordinates. The photographic values for cluster stars in common with the CCD survey (Phelps & Janes 1994) agree very closely with the CCD values, when the latter are adjusted to the present system. However, earlier photographic *UBV* photometry of cluster stars by Frolov (1979) displays systematic differences relative to the present data. Since the present survey samples a much larger number of cluster stars, no attempt was made to combine Frolov's data with the present photometry.

CCD *UBV* photometry for stars in the nuclear region of Berkeley 58 was published previously by Phelps & Janes (1994), but for this study was recalibrated using the Table 1 stars as standards. The revised photometry for cluster stars is presented in Table 4 (Appendix), where the star numbers correspond to the scheme adopted by Phelps & Janes (1994), incremented by 1000. The stars are also identified by their 2000 co-ordinates. Since the U band measurements have a much brighter limit than the B and V measures, the CCD photometry is less useful for studying the reddening in the field. But it is valuable for identifying the faint portion of the cluster main sequence.

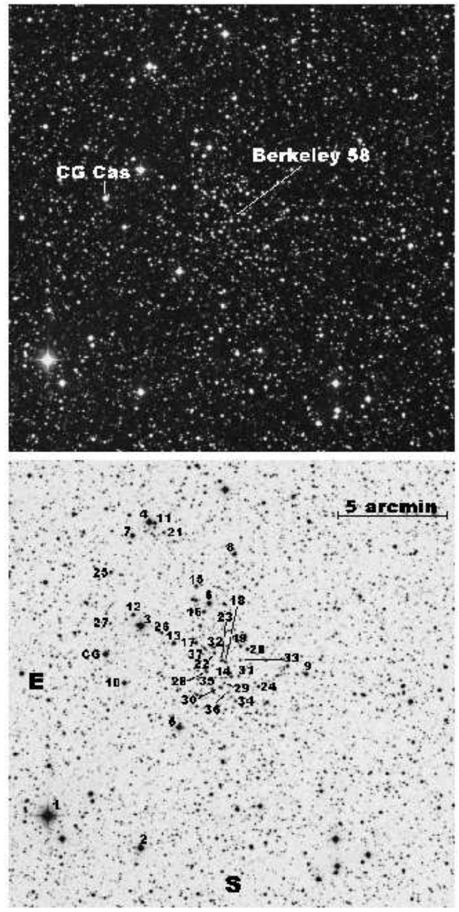

Figure 1. A finder chart for the field of Berkeley 58 from the red image of the Palomar Observatory Sky Survey. The field of view measures $20' \times 20'$ and is centred at 2000 co-ordinates: RA $= 00^{\rm h}00^{\rm m}12^{\rm s}.9$, DEC $= +60^\circ\ 56'\ 07''$. The top image depicts the location of CG Cas relative to the cluster core, the lower image identifies photoelectrically observed stars. [The National Geographic Society-Palomar Observatory Sky Atlas (POSS-I) was made by the California Institute of Technology with grants from the National Geographic Society.]

Spectroscopic imaging of bright stars in Berkeley 58 was made in 1984 July and 1985 September using the Cassegrain spectrograph on the 1.8-m Plaskett telescope of the Dominion Astrophysical Observatory. The observations, at a dispersion of 15 Å mm^{-1} and centred in the blue spectral region, were recorded photographically and later scanned for radial velocity measurement with the PDS microdensitometer at the David Dunlap Observatory of the University of Toronto (see Turner & Drilling 1984). It was also possible to estimate spectral types for the stars from the photographic spectra, with results presented in Table 1.

Table 1. Photoelectric *UBV* Data for Stars in Berkeley 58.

Star	RA(2000)	DEC(2000)	V	$B-V$	$U-B$	n	Notes
CG Cas	00 00 59.24	60 57 32.5	11.20	1.30	+1.00	15	F5–G1 I
1	00 01 21.61	60 50 21.2	7.28	0.14	−0.39	4	
2	00 00 47.68	60 48 49.8	9.80	0.27	−0.10	4	
3	00 00 46.10	60 58 46.5	9.85	1.35	+1.20	4	
4	00 00 42.77	61 03 26.1	10.02	0.58	+0.02	4	
5	00 00 32.75	60 54 11.8	10.79	2.04	+2.44	2	(K II)?
6	00 00 20.63	60 59 43.1	10.95	0.50	−0.12	4	B3–5 V[a]
7	00 00 48.46	61 02 49.5	11.49	0.46	−0.44	4	B3–5 Vnn
8	00 00 10.99	61 01 53.6	12.04	0.59	+0.26	1	
9	23 59 45.42	60 56 28.1	12.11	0.57	+0.48	3	
10	00 00 52.47	60 56 14.1	12.16	2.25	+2.51	3	
11	00 00 40.07	61 03 21.9	12.35	0.50	−0.25	4	B2.5 V
12	00 00 48.77	60 59 17.2	12.55	1.41	+1.10	1	
13	00 00 33.91	60 57 58.7	12.78	0.62	+0.09	4	
14	00 00 13.07	60 56 25.4	12.82	0.57	+0.04	4	
15	00 00 25.25	61 00 29.8	13.12	1.59	+1.50	3	
16	00 00 22.63	60 59 20.7	13.22	0.52	+0.21	5	
17	00 00 25.83	60 57 58.2	13.30	0.83	+0.55	4	
18	00 00 15.03	60 57 05.0	13.35	0.57	+0.03	4	B6 Vn
19	00 00 09.46	60 57 47.6	13.36	0.72	+0.44	2	
20	00 00 06.89	60 57 37.6	13.41	0.60	+0.11	2	
21	00 00 36.95	61 02 55.7	13.41	0.66	+0.49	3	
22	00 00 19.09	60 57 29.8	13.54	1.55	+1.39	4	
23	00 00 16.44	60 57 08.8	13.60	0.56	+0.00	4	B5:: Vnn
23	00 00 03.17	60 55 57.1	13.69	0.57	+0.10	4	B7 V
25	00 00 56.70	61 01 12.0	13.71	1.43	+1.23	2	
26	00 00 38.39	60 58 26.2	14.11	0.73	+0.59	4	
27	00 00 57.31	60 58 54.9	14.14	0.84	+0.26	4	
28	00 00 22.18	60 56 39.7	14.20	0.62	+0.19	5	
29	00 00 15.73	60 56 08.6	14.70	0.57	+0.18	4	
30	00 00 16.73	60 55 55.6	14.71	0.72	+0.35	5	double
..	...	...	15.46	0.76	...	CCD	
31	00 00 10.33	60 56 25.4	14.74	1.57	...	2	
32	00 00 19.10	60 57 44.5	14.75	0.62	+0.44	3	
33	00 00 09.64	60 57 10.1	14.91	1.02	+0.54	1	
34	00 00 11.54	60 55 19.5	15.06	1.09	...	2	
..	...	...	14.88	0.66	+0.13	CCD	
35	00 00 18.88	60 56 24.1	15.09	0.61	+0.25	4	
37	00 00 14.44	60 55 43.3	15.16	1.17	...	1	
37	00 00 23.28	60 57 27.8	15.63	0.81	+0.79	3	

[a]V654 Cas (Berdnikov 1993).

The field of the Cepheid CG Cas was also examined on archival images in the collections of Harvard College Observatory and Sternberg Astronomical Institute in order to obtain brightness estimates for the star and to construct seasonal light curves for comparison with a standard light curve constructed from photoelectric observations (Berdnikov 2007). The resulting data were used to estimate times of light maximum for the Cepheid and to track its O–C changes, the differences between observed (O) and computed (C) times of light maximum. Rate of period change, in conjunction with light amplitude, is an excellent diagnostic of the location of individual Cepheids in the instability strip (Turner et al. 2006a), such information providing an excellent parameter for comparison with what can be gleaned from information on the age of the surrounding stars provided by the cluster H-R diagram.

3 STAR COUNTS

The first step in studying Berkeley 58 involved star counts made using a photographic enlargement from a glass copy of the POSS-E plate for the field. Strip counts in several different orientations delineated the cluster centre, followed by ring counts illustrated in Fig. 2; the centre of symmetry is located at RA = $00^h00^m12^s.9$, DEC = $+60°56'07''$ (2000). The upper portion of Fig. 2 illustrates ring counts for stars detected on the 2MASS survey (Cutri et al. 2003) to the survey limit , whereas the lower portion shows star counts from the Palomar Observatory Sky Survey (POSS) E-plate to two different magnitude limits.

The counts from the 2MASS survey were made without regard for overlap with the star cluster NGC 7790, which lies $23'$ to the northwest of Berkeley 58, whereas the counts from the POSS-E plate were restricted beyond $11'$ from the cluster centre to sectors that avoided overlap with the outlying regions of NGC 7790. The effect of contamination from

Table 2. Photoelectric *UBV* Observations for CG Cassiopeiae.

HJD	V	$B-V$	$U-B$
2444849.8938	11.37	1.28	...
2444854.8655	11.53	1.36	...
2444856.8539	11.22	1.14	...
2444857.8358	11.08	1.14	...
2444857.8689	11.09	1.16	...
2445197.9177	10.92	1.04	0.74
2445205.9366	11.45	1.25	0.84
2445206.8851	11.04	1.10	0.76
2445933.8457	11.73	1.40	1.04
2445935.8748	10.99	1.08	0.85
2445937.8601	11.59	1.37	0.96
2445938.8420	11.74	1.38	1.02
2445939.8315	10.85	0.99	0.72
2445941.8773	11.55	1.35	0.93
2445942.7724	11.76	1.42	1.04

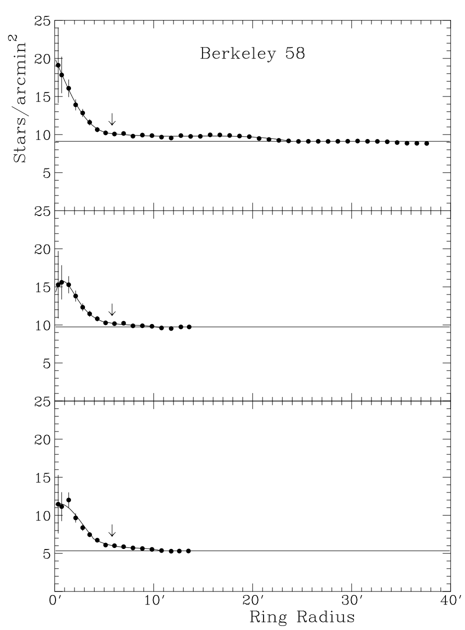

Figure 2. Star densities for the field of Berkeley 58, as measured in rings relative to the adopted cluster centre. The upper diagram contains ring counts made from the 2MASS survey, the lower two diagrams ring counts from the POSS E-plate of the field for a faint limit (middle) and a brighter limit (lower). The location of CG Cas relative to the cluster centre is indicated by an arrow.

the coronal region of NGC 7790 is detectable in the 2MASS star counts beyond roughly 12′ from the cluster centre, but because of restrictions imposed by the location of Berkeley 58 on the POSS, we were unable to establish uncontaminated star counts from the POSS-E plate beyond about 15′ from the cluster centre. Nevertheless, the two sets of counts appear to yield similar parameters for the inner regions of the cluster. Berkeley 58 is estimated to have a nuclear radius of $r_n \simeq 4'.5$ (4.0 pc) in the notation of Kholopov (1969), whereas the coronal (or tidal) radius is estimated to be $R_c \simeq 11'$ (9.7 pc) from the trends in the 2MASS star densities as well as the apparent flattening of the POSS-E star densities in the outermost rings.

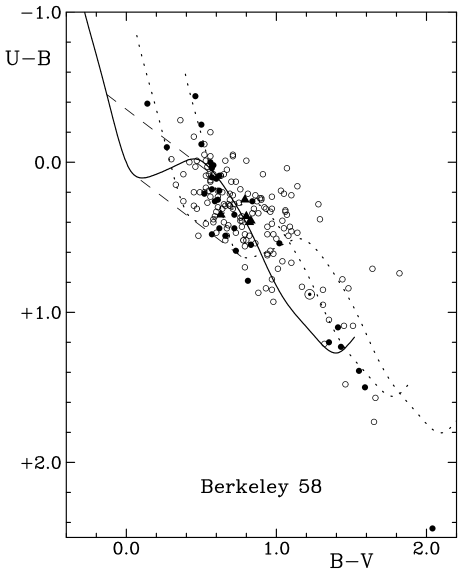

Figure 3. A *UBV* colour-colour diagram for observed Berkeley 58 stars: photoelectric observations (filled circles), photographic observations supplemented by CCD observations (open circles), CCD observations (filled triangles), and CG Cas (circled point). The intrinsic relation for main sequence stars is plotted as a solid line, with the same relation reddened by $E_{B-V} = 0.38$ and $E_{B-V} = 0.70$ shown by dotted lines. The reddening relations for stars of spectral type B6.5 V and A2 V are shown as dashed lines.

Star counts predict a total of 197±27 members brighter than the limit of the 2MASS survey lying within 5′ of the cluster centre, 487±82 members within 11′ of the cluster centre, field stars within the same regions being 715 and 4835, respectively. Field stars clearly outnumber cluster members in both regions. CG Cas is located 5′.8 from the centre of Berkeley 58, in the cluster coronal region just beyond its nuclear boundaries. Although not projected on the core of Berkeley 58, CG Cas is spatially coincident with the cluster, which occupies most of the field of Fig. 1.

4 BERKELEY 58

Fig. 3 is a *UBV* colour-colour diagram for the field of Berkeley 58 surveyed in this study, as constructed from the data of Tables 1, 3, and 4. The phase-averaged data for CG Cas are from Berdnikov (2007). A reddened sequence of B and A-type cluster members can be detected in the data, but a cluster reddening of $E_{B-V} \simeq 0.7$ places them in a section of the colour-colour diagram where they can be confused photometrically with unreddened, foreground, G-type stars. For that reason it becomes essential to make the process of photometric identification of likely spectral classes for individual stars as reliable as possible, through the use of a well-established interstellar extinction relation. The spectral types obtained for six of the B-type, photoelectrically-observed, cluster stars imply a reddening law for Berkeley 58 described by $E_{U-B}/E_{B-V} = 0.75$, along with a small curvature term (Turner 1989), identical to the reddening slope found previously for star clusters spatially adjacent to Berkeley 58 (Turner 1976b). Berkeley 58 stars were therefore dereddened with such a relationship, except for late-type

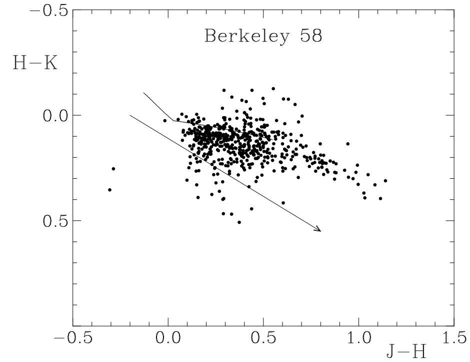

Figure 4. A 2MASS colour-colour diagram, *H–K* versus *J–H*, for stars examined in the field of Berkeley 58, without regard to the uncertainties in the observations (Cutri et al. 2003). The intrinsic relation for main sequence stars is plotted as a solid line, as derived from the observed colours of standard stars and stars in clusters of uniform reddening. The direction of reddening in the 2MASS system is indicated.

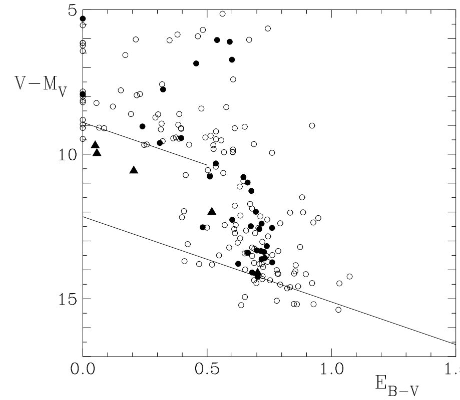

Figure 5. A variable-extinction diagram for observed Berkeley 58 stars, with symbols as in Fig. 3. Reddening relations of slope $R = A_V/E_{B-V} = 2.95$ are shown corresponding to distances of $d \simeq 600$ pc ($V_0 - M_V = 8.9$) and $d \simeq 2700$ pc ($V_0 - M_V = 12.16$).

stars where a steeper relationship was adopted, dependent upon the likely intrinsic colours of the stars.

The Fig. 3 data indicate an absence of any unreddened O, B, or A-type stars in the observed sample. That feature is confirmed by available 2MASS data for the observed stars (Cutri et al. 2003), which are depicted in the *JHK* colour-colour diagram of Fig. 4. An intrinsic relation for main-sequence stars in the 2MASS system was constructed from 2MASS observations of unreddened standard stars and stars in open clusters of uniform reddening (e.g., Turner 1996b), adjusted with a reddening slope $E_{H-K}/E_{J-H} = 0.55$, as derived from reddened stars of known spectral type. The number of cluster stars with *U*-band observations is a small fraction of the total sample, so Fig. 4 contains many more stars than Fig. 3. The selection of 2MASS data was also not restricted according to the magnitude of cited uncertainties in the data, so several points in Fig. 4 display unusually large scatter. It seems clear, however, that the sample of cluster stars surveyed consists mainly of stars reddened by $E_{J-H} \geqslant 0.1$, which corresponds to $E_{B-V} \geqslant 0.36$.

The correleation of reddening with distance towards Berkeley 58 was established from the available *UBV* photometry by dereddening the colours for individual stars in conjunction with a copy of the POSS field on which derived colour excesses E_{B-V} were recorded as they were obtained, with multiple solutions resolved by reference to the reddenings for spatially adjacent stars as well as by the reddenings derived for the stars from their 2MASS colours (Fig. 4). In most cases the smaller *JHK* reddening of stars relative to those obtained from *UBV* colours was sufficient to resolve questions about likely intrinsic colours for the stars, but there were a number of ambiguous cases where the data from the two surveys yielded disparate solutions, *e.g.* 2MASS colours implying an early spectral type and *UBV* colours implying a late spectral type. Such cases were unimportant in the final analysis, but are curious nevertheless.

Distance moduli were calculated for individual stars by adoption of zero-age main sequence (ZAMS) values of M_V (Turner 1976a, 1979), so the values systematically underestimate V–M_V for unresolved binaries and evolved stars. The resulting scatter in the variable-extinction diagram of Fig. 5 therefore contains a systematic component towards small values of V–M_V. Within such constraints, it is possible to discern certain trends in the data, such as the lack of any significant reddening out to distances of ~ 600 pc ($V_0 - M_V = 8.9$), with a reddening of $E_{B-V} \geqslant 0.4$ beyond that to distances of ~ 2700 pc ($V_0 - M_V = 12.16$) or more. At the Galactic location of CG Cas ($l = 116^\circ.845$, $b = -1^\circ.315$), a more encompassing survey by Neckel & Klare (1980) implies a similar trend, with the reddening beginning at distances of $\sim 400 - 900$ pc. Apparently the main extinction for stars in the direction of Berkeley 58 occurs near the far side of the local spiral arm feature.

But the picture is not that simple. When the derived reddenings are compared star-for-star in the field of Berkeley 58, there are no obvious trends with spatial location, and trends with distance are difficult to establish without highly accurate luminosities for the observed stars. It can be surmised that there is additional reddening occurring on the near side of the Perseus spiral arm, given the nature of the scatter in the colour excesses. Likely members of Berkeley 58 generally have reddenings of $E_{B-V} \simeq 0.70$, with larger values possibly arising from circumstellar extinction, particularly for late B-type stars where rapid rotation is common (e.g., Turner 1993, 1996a). An identical feature is observed in the adjacent cluster NGC 7790 (Takala 1988). A lower envelope trend for the reddened stars in Fig. 5 implies a ratio of total-to-selective extinction for the field of $R = A_V/E_{B-V} = 2.95 \pm 0.30$ from least squares and non-parametric analyses. The value is consistent with previous studies of clusters in this region of the Galaxy (Turner 1976b), as well as with a value of $R \simeq 2.95$ expected for local extinction described by a reddening slope of 0.75 (Turner 1996a). For subsequent calculations a value of $R = 2.95$ was adopted, the exact choice affecting estimates of distance but not the derived luminosity for CG Cas as a cluster member.

An observational colour-magnitude diagram for the sampled atars is presented in Fig. 6, with a ZAMS plotted for V–$M_V = 14.29$, the apparent distance modulus at $E_{B-V} = 0.70$ for points on the lower relation of Fig. 5. Such parameters provide a reasonable fit to the data, but there remain anomalies requiring further examination. For

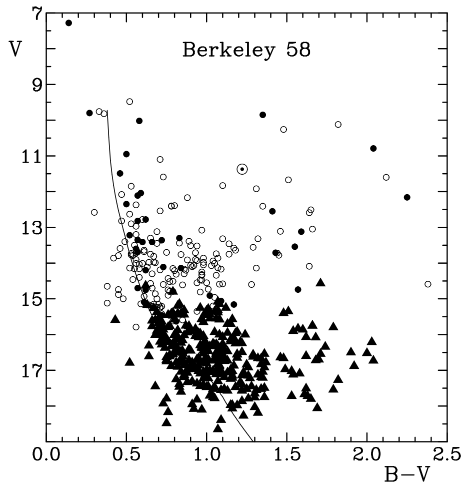

Figure 6. A colour-magnitude diagram for Berkeley 58 from all observations: photoelectric (filled circles), photographic (open circles), and CCD (triangles) data. CG Cas is the circled point. The ZAMS is depicted for $E_{B-V} = 0.70$ and $V–M_V = 14.29$.

example, Fig. 6 contains reddened B-type stars more luminous than the turnoff magnitude for a cluster containing CG Cas, a point also indicated in Fig. 3, where dashed relations indicate reddening lines for B6.5 V and A2 V stars, the former corresponding to the expected turnoff color $[(B-V)_0 = -0.13]$ for stars associated with a $4^{\rm d}.37$ Cepheid (Turner 1996c). Clearly the field contains a number of stars younger than the expected evolutionary age of CG Cas.

Such complications may be endemic to the field of both Berkeley 58 and NGC 7790, where the line of sight crosses the interarm region between the Sun and portions of the local spiral feature, then intercepts the Perseus spiral arm with a marked increase in space density for young B-type stars and young-to-intermediate age star clusters. The separation of spiral arm stars from cluster members is difficult but achievable, since the radial velocities for CG Cas and Berkeley 58 stars listed in Table 5 imply a conspicuous velocity difference between the cluster and spiral arm stars. The anomalously young B stars noted above are objects like stars 6 (V654 Cas), 7, and possibly 24, which have systematically more positive velocities than likely cluster members: stars 11, 18, and 23, which have radial velocities close to the systemic velocity of CG Cas (see Fig. 7, which includes radial velocity measurements from Joy 1937; Metzger et al. 1991; Gorynya et al. 1998). Except for star 11, which may be anomalous, stars with radial velocities close to that of CG Cas also have spectral types near the expected B6.5 V turnoff. Unfortunately it is not possible to identify fainter cluster members by the same technique, given the bright limit for the present radial velocity survey. Follow-up observations would be useful in that regard.

The complications arising from contamination of the cluster field by young stars in the Perseus arm and likely circumstellar reddening for late B-type members were addressed by identifying unaffected cluster stars from their reddenings, which are close to $E_{B-V}(\rm B0) = 0.70$. The field of the CCD survey near the cluster centre was found to exhibit a mean reddening of $E_{B-V}(\rm B0) = 0.697 \pm 0.025$, that for the region of CG Cas a mean reddening of $E_{B-V}(\rm B0) =$

Table 5. Radial Velocity Data for Berkeley 58 Stars.

Star	HJD	V_R (km s^{-1})	Adopted V_R (km s^{-1})
CG Cas	2445906.955	-74.5 ± 3.8	
	2445908.942	-78.3 ± 1.4	
	2445909.944	-98.4 ± 3.0	
	2445910.933	-84.8 ± 1.3	
	2445911.935	-73.0 ± 1.8	
	2445912.923	-63.9 ± 1.7	
	2446326.874	-72.4 ± 2.3	
	2446327.907	-65.5 ± 3.7	
	2446328.910	-100.1 ± 1.2	
	2446330.890	-70.5 ± 1.2	
	2446331.881	-60.5 ± 2.3	-78.8
6	2445908.961	-13.3 ± 3.5	
	2446326.940	-88.3 ± 4.1	
	2446327.955	-47.7 ± 6.5	-52.3
7	2445909.963	-57.6 ± 5.3	
	2446327.942	-61.3 ± 2.9	
	2446331.020	-68.7 ± 4.2	-62.7
11	2445910.956	-80.7 ± 1.2	
	2446330.919	-70.9 ± 5.1	
	2446331.909	-70.4 ± 3.3	-79.1
18	2445911.760	-82.1 ± 10.1	
	2446326.914	-81.6 ± 3.3	-81.6
23	2446328.955	-77.8 ± 13.0	-77.8
24	2446330.972	-69.8 ± 8.5	-69.8
		Cluster Mean =	-79.4 ± 1.0

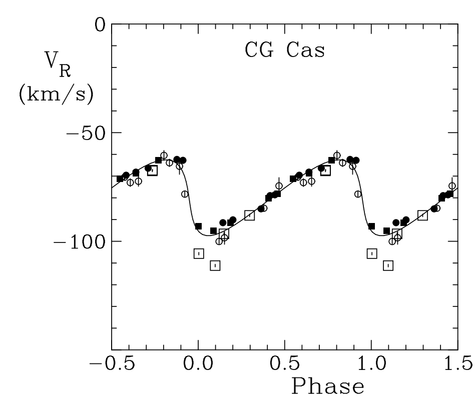

Figure 7. The radial velocity variations of CG Cas, with cited uncertainties, as measured in this paper (open circles), from Metzger et al. (1991) and Gorynya et al. (1998) (filled circles), and from Joy (1937) (open squares). The curve is a simple spectroscopic binary solution to the data from the first three data sets, the data from Joy (1937) exhibiting systematic deviations near velocity minimum.

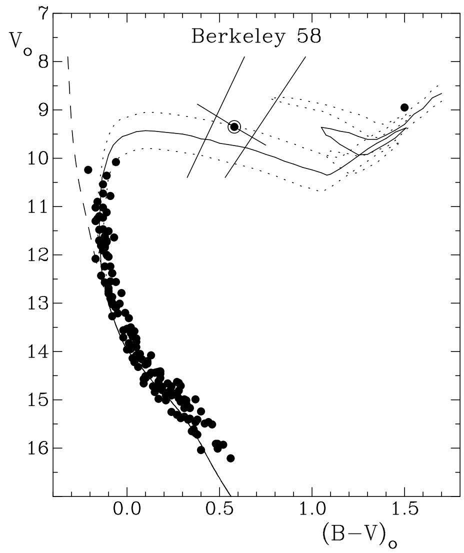

Figure 8. A reddening free colour-magnitude diagram for Berkeley 58. The dashed curve represents the ZAMS for $V_0 - M_V = 12.40$, and the solid line with dotted lines on either side represents an isochrone from Meynet et al. (1993) for $\log \tau = 8.0 \pm 0.1$. The range of light variations for CG Cas are depicted, as are the observational boundaries for the Cepheid instability strip. The red object on the evolved giant sequence is star 5.

0.685 ± 0.022. Stars with full UBV data were identified as likely cluster members on the basis of reddenings comparable to or larger than those values, while stars near the cluster centre lacking U-band data were assumed to have B0 star colour excesses as above, but intrinsic colours adjusted for the spectral type dependence of reddening (see Fernie 1963). A-type dwarfs can suffer complications arising from the effects of rotation on their stellar continua and UBV colours (Turner et al. 2006b), so the adoption of space reddenings for such stars may circumvent potential biases introduced by dereddening their colours to the intrinsic relation for zero-age zero-rotation main sequence stars. The resulting reddening-corrected colour-magnitude diagram for the cluster is plotted in Fig. 8 for 145 likely members, along with CG Cas and its light variations and star 5, which is considered to be a potential K giant member. The reddening for CG Cas corrected for its colour is $E_{B-V} = 0.64 \pm 0.02$. A photometric reddening could be obtained from the BVI_c observations of Henden (1996) (see Laney & Caldwell 2007), but a field reddening was adopted as a precaution against potential bias towards large-amplitude Cepheids lying near the centre of the instability strip (unnecessary in the present case, as it turns out).

The distance to Berkeley 58 is established by 40 of its A-type ZAMS members, which yield a value of $V_0 - M_V = 12.40 \pm 0.12$ s.d., corresponding to a distance of 3026 ± 166 pc. Except for star 11, which is conceivably a rapid rotator observed nearly pole-on, the bluest cluster stars correspond to spectral type B6 with $(B–V)_0 = -0.16$. A comparison with stellary evolutionary models (Meynet et al. 1993) implies a cluster age of $10 \pm 1 \times 10^7$ years ($\log \tau = 8.0 \pm 0.05$). The corresponding mass of cluster stars falling at the tip of the main-sequence red turnoff (RTO) is $5.4 M_{\odot}$ (Meynet et al. 1993).

5 CG CASSIOPEIAE

The systemic radial velocity of CG Cas (Table 5) is a close match to the mean velocity of Berkeley 58 derived from likely cluster members 11, 18, and 23, and the evolutionary age of the cluster closely matches what is predicted for the pulsation period of the Cepheid (Turner 1996c). The luminosity of CG Cas as a likely member of Berkeley 58 is $\langle M_V \rangle = -3.06 \pm 0.12$, which matches a value of $\langle M_V \rangle = -3.04$ predicted with a Cepheid period-radius relation and the inferred effective temperature of CG Cas ($\log T_{\rm eff} = 3.775$) from its derived intrinsic colour (Turner & Burke 2002). The case for membership of CG Cas in Berkeley 58 is very strong.

The exact evolutionary status of CG Cas can be established from the direction and rate of its period changes (Turner et al. 2006a), in conjunction with its large blue light amplitude of $\Delta B = 1.22$ (Berdnikov 2007). The period changes for CG Cas were established here from examination of archival photographic plates in the Harvard and Sternberg collections, as well as from an analysis of new and existing photometry for the star. A working ephemeris for CG Cas based upon the available data was:

$$\mathrm{JD_{max}} = 2432436.94 + 4.3656292\,E,$$

where E is the number of elapsed cycles. An extensive analysis of all available observations produced the data summarized in Table 6, which lists the results for different epochs, the type of data analyzed (PG = photographic, VIS = visual telescopic observations, B = photoelectric B, and V = photoelectric V), the number of observations used to establish the times of light maximum, and the source of the observations, in addition to the temporal parameters. The data are plotted in Fig. 9.

A regression analysis of the O–C data of Table 6 produced a parabolic solution for the ephemeris defined by:

$$\mathrm{JD_{max}} = 2432436.9493(\pm 0.0080)$$

$$+4.3656289(\pm 0.0000024)\,E + 1.1757(\pm 0.0983) \times 10^{-7}\,E^2,$$

which is plotted in Fig. 8. The parabolic trend corresponds to a period increase of $+0.170 \pm 0.014$ s yr^{-1} ($\log \dot{P} = -0.770 \pm 0.036$), a value typical of Cepheids lying slightly blueward of the centre of the instability strip and in the third crossing. The location of CG Cas in Fig. 8 relative to the observational boundaries of the Cepheid instability strip (Turner et al. 2006b) is consistent with that conclusion, although the stellar evolutionary models seem to require adjustments (metallicity, mixing of surface layers?) to match the observations.

6 DISCUSSION

The case for potential membership of the Cepheid CG Cas in the sparse open cluster Berkeley 58 has been studied using photometric (pe, pg, CCD) observations, spectroscopy (V_R, spectral types), star counts, and O–C data for the Cepheid. The cluster Berkeley 58 is particularly difficult to separate from the young stars of the Perseus spiral arm, which raises concerns about future studies of distant open cluster calibrators for the Cepheid PL relation. Careful analysis of the available data leads to a cluster reddening of $E_{B-V}(\mathrm{B0}) = 0.70$, a distance of 3.03 ± 0.17 kpc, and an age

Table 6. Times of Maximum Light for CG Cas.

HJD_{max}	$\pm\sigma$	Band	Epoch (E)	O–C (phase)	Observations (n)	Reference
2413407.3442	0.0292	PG	–4359	+0.1714	55	This paper (Harvard)
2415144.8677	0.0428	PG	–3961	+0.1746	7	This paper (SAI)
2416314.8382	0.0338	PG	–3693	+0.1566	72	This paper (Harvard)
2417572.0492	0.1070	PG	–3405	+0.0664	11	This paper (SAI)
2419794.1315	0.0336	PG	–2896	+0.0436	63	This paper (Harvard)
2423788.6688	0.0271	PG	–1981	+0.0304	98	This paper (Harvard)
2426102.4299	0.0196	PG	–1451	+0.0082	128	This paper (Harvard)
2426940.6916	0.0567	VIS	–1259	+0.0691	46	Lange (1933)
2428023.3553	0.0571	PG	–1011	+0.0569	19	This paper (SAI)
2428455.5134	0.0271	PG	–912	+0.0177	92	This paper (Harvard)
2429568.7382	0.0559	PG	–657	+0.0071	28	This paper (SAI)
2430847.7814	0.0321	PG	–364	–0.0790	81	This paper (Harvard)
2431576.8823	0.0854	PG	–197	–0.0381	17	Erleksova (1961)
2433100.4046	0.0430	PG	+152	–0.1203	59	This paper (Harvard)
2433183.4566	0.0308	PG	+171	–0.0152	37	This paper (SAI)
2433371.0678	0.0848	PG	+214	–0.1261	23	Erleksova (1961)
2434117.6643	0.0350	PG	+385	–0.0521	25	This paper (SAI)
2435174.1804	0.0285	PG	+627	–0.0182	74	This paper (SAI)
2435379.4291	0.0443	PG	+674	+0.0459	10	Romano (1959)
2435619.5498	0.1388	PG	+729	+0.0570	19	Erleksova (1961)
2435837.7841	0.0168	PG	+779	+0.0099	18	Zonn & Semeniuk (1959)
2436802.5876	0.0070	B	+1000	+0.0094	13	Oosterhoff (1960)
2436802.6183	0.0119	V	+1000	+0.0401	15	Oosterhoff (1960)
2436933.5492	0.0054	B	+1030	+0.0021	22	Bahner et al. (1962)
2436937.9440	0.0085	V	+1031	+0.0313	23	Bahner et al. (1962)
2438666.6957	0.0174	PG	+1427	–0.0061	41	This paper (SAI)
2439077.0406	0.0299	PG	+1521	–0.0303	16	This paper (SAI)
2440268.8346	0.0241	PG	+1794	–0.0530	24	This paper (SAI)
2441146.3548	0.0121	PG	+1995	–0.0242	95	This paper (SAI)
2441866.7282	0.0142	PG	+2160	+0.0204	55	This paper (SAI)
2442355.6761	0.0178	PG	+2272	+0.0178	47	This paper (SAI)
2442862.0722	0.0159	PG	+2388	+0.0010	74	This paper (SAI)
2443045.5091	0.0058	V	+2430	+0.0815	71	Chekanikhina (1982)
2443957.9197	0.0206	PG	+2639	+0.0756	25	This paper (SAI)
2444844.1310	0.0099	B	+2842	+0.0643	9	Berdnikov (1986)
2444852.8817	0.0150	V	+2844	+0.0837	11	Berdnikov (1986)
2445189.0177	0.0117	B	+2921	+0.0663	8	Berdnikov (1986)
2445189.0509	0.0074	V	+2921	+0.0995	8	Berdnikov (1986)
2445394.1872	0.0098	B	+2968	+0.0512	14	This paper
2445429.1355	0.0115	V	+2976	+0.0745	15	This paper
2445883.1690	0.0061	B	+3080	+0.0826	8	Berdnikov (1986)
2445883.1870	0.0086	V	+3080	+0.1006	8	Berdnikov (1986)
2447760.4530	0.0042	B	+3510	+0.1461	39	Berdnikov (1992a)
2447760.4823	0.0059	V	+3510	+0.1754	39	Berdnikov (1992a)
2448118.4162	0.0060	B	+3592	+0.1277	18	Berdnikov (1992b)
2448118.4546	0.0085	V	+3592	+0.1661	18	Berdnikov (1992b)
2448515.7127	0.0043	B	+3683	+0.1520	20	Berdnikov (1992c)
2448515.7328	0.0052	V	+3683	+0.1721	20	Berdnikov (1992c)
2451458.2287	0.0152	V	+4357	+0.2341	27	Wozniak et al. (2004)

of $10\pm1\times10^7$ years. CG Cas is a likely member on the basis of radial velocity, location outside the cluster nucleus within the cluster coronal region, evolutionary status indicated by its period changes and light amplitude, and implied luminosity. It becomes an important Cepheid calibrator lying near the centre of the instability strip.

It may seem unusual that many potential Cepheid calibrators lie in cluster coronae rather than cluster nuclear regions (Turner 1985), but a possible explanation relates to two dynamical lines of evidence. First, massive cluster members lie preferentially in outer regions of clusters (Burki 1978), possibly because of how proto-cluster interstellar clouds fragment into proto-stars. Second, as indicated by colour-magnitude diagrams for NGC 654 (Stone 1980) and other young clusters (Turner 1996b), cluster nuclear regions tend to be dominated by rapidly rotating stars, possibly the result of merged binary systems, and other close binaries, in which case potential Cepheid progenitors are less likely to evolve to the dimensions typical of pulsating variables because of restrictions on their dimensions engendered by po-

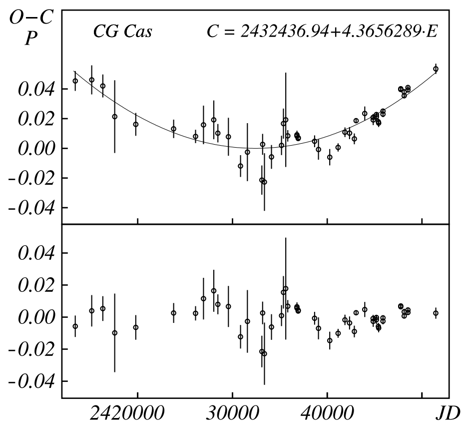

Figure 9. The differences between observed (O) and computed (C) times of light maximum for CG Cas, computed in units of pulsation phase. The upper diagram shows the actual O–C variations with their uncertainties, the lower diagram the residuals from the calculated parabolic evolutionary trend.

tential physical companions. The case of CG Cas in Berkeley 58 appears to be yet another example of the effect.

ACKNOWLEDGEMENTS

The present study was supported by research funding awarded through the Natural Sciences and Engineering Research Council of Canada (NSERC), through the Small Research Grants program of the American Astronomical Society, through the Russian Foundation for Basic Research (RFBR), and through the program of Support for Leading Scientific Schools of Russia. We are endebted to Ron Lyons for scanning the radial velocity plates used in this study, and to the director of Harvard College Observatory for access to the plate stacks.

REFERENCES

Bahner K., Hiltner W. A., Kraft, R. P., 1962, ApJS, 6, 319
Berdnikov L. N., 1986, Peremen. Zv., 22, 369
Berdnikov L. N., 1992a, A&AT, 2, 107
Berdnikov L. N., 1992b, A&AT, 2, 157
Berdnikov L. N., 1992c, Astr. Lett., 18, 130
Berdnikov L. N., 1993, Peremen. Zv., 23, 80
Berdnikov L. N., 2007, http://www.sai.msu.ru/groups/cluster/cep/phe
Burki G., 1978, A&AS, 62, 159
Chekanikhina O. A., 1982, Bull. Astrophys. Inst. AN Tadj. SSR, No. 71, 25
Cutri R. M., Skrutskie M. F., van Dyk S., et al., 2003, The IRSA 2MASS All-Sky Point Source Catalog of Point Sources, NASA/IPAC Infrared Science Archive
Efremov Y. N., 1964a, Peremen. Zv., 15, 242
Efremov Y. N., 1964b, Astr. Tsirk., No. 292, 3
Erleksova G. E., 1961, Bull. Astrophys. Inst. AN Tadj. SSR, No. 30, 28
Fernie J. D., 1963, AJ, 68, 780
Frolov V. N., 1974, Astr. Tsirk., No. 848, 1
Frolov V. N., 1977, Izv. Glavnaia Astr. Obs. Pulkovo, No. 195, 80
Frolov V. N. 1979, Izv. Glavnaia Astr. Obs. Pulkovo, No. 196, 69
Gorynya N. A., Samus N. N., Sackhov M. E., Rastorguev A. S., Glushkova E. V., Antipin S. V., 1998, Pis'ma Azh, 24, 939
Henden A. A., 1996, AJ, 112, 2757
Irwin J. B., 1955, MNASSA, 14, 38
Irwin J. B., 1958, AJ, 63, 197
Joy A. E., 1937, ApJ, 86, 363
Kholopov P. N., 1956, Peremen. Zv., 11, 325
Kholopov P. N., 1969, SvA, 12, 625
Kovalenko V. M., 1968, Astr. Tsirk., No. 473, 2
Kraft R. P., 1957, ApJ, 126, 225
Laney C. D., Caldwell J. A. R., 2007, MNRAS, 377, 147
Lange G., 1933, Leningrad Univ. Astr. Obs. Bull., No. 2, 9
Meynet G., Mermilliod J.-C., Maeder A., 1993, A&AS, 98, 477
Metzger M. R., Caldwell J. A. R., McCarthy J. K., Schechter P. L., 1991, ApJS, 76, 803
Neckel Th., Klare G., 1980, A&AS, 42, 251
Oosterhoff P. Th., 1960, BAN, 15, 199
Phelps R. L., Janes K. A., 1994, ApJS, 90, 31
Romano G., 1959, Pub. Osserv. Astr. Padova, No. 116, 3
Sandage A., 1958, ApJ, 128, 150
Stone R. C., 1980, PASP, 92, 426
Setteducati A. F., Weaver H. F., 1962, Newly Found Star Clusters, Radio Astron. Lab., Univ. California, Berkeley
Takala J. M., 1988, MSc thesis, Saint Mary's Univ.
Tifft W. G., 1959, ApJ, 129, 241
Turner D. G., 1976a, AJ, 81, 97
Turner D. G., 1976b, AJ, 81, 1125
Turner D. G., 1979, PASP, 91, 642
Turner D. G., 1985, in Madore B. F., ed., IAU Colloq. 82, Cepheids: Theory and Observations, Cambridge Univ. Press, Cambridge, p. 209
Turner D. G., 1989, AJ, 98, 2300
Turner D. G., 1992, AJ, 104, 1865
Turner D. G., 1993, A&AS, 97, 755
Turner D. G., 1996a, in Milone E. F., Mermilliod J.-C., eds., The Origins, Evolution, and Destinies of Binary Stars in Clusters, ASP Conf. Series 90, p. 382
Turner D. G., 1996b, in Milone E. F., Mermilliod J.-C., eds., The Origins, Evolution, and Destinies of Binary Stars in Clusters, ASP Conf. Series 90, p. 443
Turner D. G., 1996c, JRASC, 90, 82
Turner D. G., Burke, J. F., 2002, AJ, 124, 2931
Turner D. G., Drilling J. S., 1984, PASP, 96, 292
Turner D. G., Welch G. A., 1989, PASP, 101, 1038
Turner D. G., Forbes D., Pedreros M., 1992, AJ, 104, 1132
Turner D. G., Mandushev G. I., Forbes D., 1994, AJ, 107, 1796
Turner D. G., Abdel-Sabour Abdel-Latif M., Berdnikov L. N., 2006a, PASP, 118, 410
Turner D. G., Usenko I. A., Kovtyukh V. V., 2006b, Observatory, 126, 207
van den Bergh S., 1957, ApJ, 126, 323
Wozniak P. R., Vestrand W. T., Akerlof C. W., et al., 2004, AJ, 127, 2436
Zonn W., Semeniuk I., 1959, Acta Astr., 9, 141

APPENDIX

Table 3. Photographic *UBV* Data for Stars in Berkeley 58.

Star	RA(2000)	DEC(2000)	V	$B-V$	$U-B$	Star	RA(2000)	DEC(2000)	V	$B-V$	$U-B$
101	23 59 36.09	+60 49 01.9	9.48	0.52	−0.05	179	00 01 21.27	+60 53 30.5	14.01	0.60	+0.47
102	00 00 13.86	+61 04 47.4	9.76	0.33	+0.15	180	23 59 56.23	+60 56 25.0	14.03	0.58	+0.08
103	00 01 16.38	+60 49 18.1	9.82	0.36	−0.28	181	23 58 53.10	+60 57 05.6	14.05	0.98	+0.93
104	23 59 24.28	+60 48 18.3	10.12	1.82	+0.74	182	23 59 10.64	+60 51 55.7	14.06	0.90	+0.25
105	23 59 35.71	+60 47 49.6	10.26	1.48	+0.84	183	23 59 17.01	+60 51 12.5	14.07	1.03	+0.19
106	00 00 03.42	+60 50 36.1	11.10	0.71	−0.05	184	23 59 47.40	+60 48 27.0	14.07	0.92	+0.30
107	23 59 36.15	+60 47 33.1	11.59	0.73	+0.13	185	23 59 50.39	+60 58 39.3	14.09	1.64	...
108	23 59 42.73	+60 47 16.1	11.60	2.12	+2.67	186	00 00 49.32	+60 48 06.5	14.10	0.91	+0.08
109	23 59 07.11	+60 55 06.8	11.67	1.51	+1.09	187	00 00 24.36	+60 55 35.8	14.11	0.63	+0.09
110	00 01 05.72	+60 51 17.7	11.83	1.10	+0.67	188	23 59 49.10	+60 50 32.7	14.13	1.07	+0.35
111	00 00 11.91	+60 50 28.6	11.85	0.53	+0.17	189	23 58 57.51	+60 58 24.8	14.14	1.31	+0.85
112	00 01 20.84	+60 52 34.9	11.92	1.31	+0.95	190	23 59 22.80	+60 57 04.3	14.14	0.52	−0.12
113	00 01 21.00	+61 00 48.4	12.08	0.47	+0.31	191	23 59 05.78	+61 01 43.6	14.15	0.79	+0.70
114	00 01 10.16	+61 03 50.0	12.17	0.88	+0.34	192	23 59 46.99	+61 03 27.0	14.16	0.58	+0.38
115	00 01 20.63	+60 55 32.1	12.37	0.56	+0.12	193	00 00 55.95	+61 03 02.4	14.16	0.55	+0.19
116	00 00 07.17	+60 48 48.4	12.39	0.80	+0.52	194	00 00 04.13	+60 51 51.7	14.17	0.86	+0.54
117	23 58 53.91	+60 56 37.2	12.40	0.78	+0.52	195	00 00 37.31	+60 46 36.1	14.17	1.09	+0.43
118	23 59 10.07	+60 55 48.6	12.41	0.78	+0.52	196	23 59 37.23	+61 01 47.2	14.19	0.71	−0.04
119	23 59 40.81	+60 51 12.4	12.41	1.35	+1.05	197	00 01 14.97	+60 54 01.9	14.20	0.87	+0.26
120	00 00 24.15	+61 05 54.4	12.51	1.65	+1.73	198	23 59 07.54	+60 59 40.0	14.21	0.80	−0.01
121	00 00 16.78	+60 52 39.3	12.54	0.71	+0.22	199	23 59 49.51	+60 59 23.1	14.25	0.97	+0.85
122	00 01 05.00	+60 50 58.3	12.58	0.30	−0.02	200	00 00 26.46	+60 50 28.7	14.30	0.66	+0.52
123	23 59 11.61	+61 02 04.7	12.59	1.64	+0.71	201	00 00 51.81	+60 46 54.6	14.30	0.86	+0.22
124	23 59 43.07	+61 03 17.7	12.63	0.52	+0.20	202	00 00 23.33	+60 51 42.1	14.31	0.81	+0.21
125	23 59 06.63	+60 53 17.9	12.78	0.60	+0.33	203	23 59 34.32	+60 59 24.9	14.32	0.97	+0.31
126	00 01 05.84	+60 59 50.1	12.82	0.47	−0.01	204	23 59 17.67	+60 54 45.5	14.34	1.06	+0.33
127	00 01 33.08	+60 53 08.0	12.90	0.53	+0.41	205	00 00 11.83	+61 05 55.5	14.34	0.97	+0.41
128	00 00 57.98	+61 04 02.5	12.97	0.56	−0.20	206	23 59 41.42	+60 51 28.7	14.40	0.58	+0.40
129	00 00 25.44	+60 59 52.4	13.05	1.66	+1.57	207	00 00 25.66	+60 50 43.7	14.43	0.76	+0.18
130	23 59 03.83	+60 51 31.8	13.08	0.97	+0.23	208	23 59 42.89	+61 02 29.1	14.46	0.54	+0.03
131	23 58 54.24	+60 54 15.1	13.11	1.46	+1.48	209	00 00 58.82	+60 55 01.6	14.47	0.96	+0.59
132	00 00 26.72	+60 59 55.4	13.12	0.69	+0.29	210	00 00 00.99	+61 00 51.4	14.48	0.97	+0.78
133	23 59 19.28	+60 50 11.7	13.20	0.56	−0.04	211	00 01 25.15	+61 02 11.0	14.51	0.79	+0.56
134	23 59 24.57	+60 55 27.9	13.30	0.65	+0.40	212	23 59 23.62	+60 59 41.4	14.52	0.77	+0.36
135	23 59 59.65	+61 04 09.7	13.32	1.32	+1.21	213	00 00 26.84	+60 49 40.7	14.55	1.00	+0.51
136	00 00 27.04	+60 46 43.8	13.32	1.10	+0.22	214	00 01 21.95	+61 02 29.5	14.55	0.94	+0.62
137	00 00 28.97	+60 47 58.6	13.39	0.89	+0.24	215	00 00 25.83	+60 55 38.0	14.57	0.65	+0.28
138	00 00 21.24	+60 51 10.6	13.40	0.49	+0.20	216	23 59 06.22	+60 53 57.6	14.58	1.10	+0.46
139	00 01 16.05	+61 02 45.5	13.44	0.83	+0.55	217	00 01 18.21	+61 01 23.9	14.59	1.08	+0.49
140	23 59 41.35	+61 05 46.4	13.45	0.69	+0.25	218	00 00 16.19	+60 53 17.5	14.59	2.38	...
141	23 58 50.90	+60 54 37.2	13.46	1.14	+0.16	219	23 59 22.49	+60 52 00.0	14.60	1.28	+0.28
142	00 00 15.19	+60 59 41.4	13.50	0.55	+0.08	220	00 00 01.21	+60 57 39.2	14.60	0.73	+0.47
143	00 01 38.02	+60 57 11.3	13.51	0.90	+0.24	221	00 00 28.99	+60 52 57.1	14.61	0.85	+0.31
144	00 00 19.83	+60 49 11.5	13.52	0.94	+0.48	222	00 00 53.50	+60 55 22.0	14.65	0.38	+0.08
145	23 59 48.55	+60 46 45.3	13.56	1.29	+0.38	223	00 00 28.35	+61 05 20.9	14.70	0.66	−0.01
146	00 00 24.12	+60 58 43.8	13.58	1.17	+0.83	224	23 59 58.59	+60 54 09.2	14.73	1.01	+0.71
147	00 01 14.18	+60 56 32.2	13.59	0.46	+0.03	225	00 01 16.76	+60 54 30.9	14.74	0.45	−0.17
148	23 59 24.83	+60 59 52.9	13.64	1.18	...	226	00 00 18.03	+60 51 36.5	14.75	0.76	+0.37
149	00 00 07.41	+61 00 24.1	13.64	0.61	+0.23	227	23 59 32.73	+60 59 21.3	14.79	0.79	+0.48
150	00 00 01.78	+60 48 57.5	13.68	0.61	+0.30	228	00 00 10.51	+60 58 01.8	14.79	0.77	+0.43
151	23 58 55.65	+60 52 55.3	13.70	0.75	+0.27	229	23 59 40.12	+60 57 06.2	14.81	0.96	+0.33
152	23 59 09.72	+60 55 33.4	13.71	0.93	+0.31	230	00 00 20.17	+60 55 54.3	14.86	0.68	+0.28
153	23 59 52.24	+60 56 50.2	13.72	0.56	+0.13	231	00 00 02.48	+60 54 42.4	14.88	0.45	+0.20
154	00 00 49.48	+61 03 45.2	13.72	1.44	+0.78	232	23 59 49.71	+60 53 31.9	14.90	0.76	+0.39
155	00 01 38.95	+60 57 40.8	13.73	0.53	−0.01	233	00 00 04.01	+60 54 47.8	14.93	0.61	+0.19
156	00 00 27.09	+61 05 48.8	13.74	1.06	+0.32	234	00 00 33.02	+60 55 51.9	14.96	1.05	+0.44
157	23 59 34.31	+60 49 44.5	13.75	1.14	+0.47	235	00 00 09.83	+60 54 30.1	15.00	0.69	+0.21
158	00 00 44.24	+60 46 52.3	13.75	0.65	+0.08	236	00 00 44.08	+61 05 04.7	15.00	0.48	+0.49
159	00 00 31.53	+60 46 32.0	13.76	0.84	+0.34	237	00 00 09.76	+61 05 34.5	15.12	0.38	+0.26
160	00 00 38.87	+60 53 10.0	13.77	0.53	+0.09	238	23 59 42.48	+60 56 18.8	15.14	0.59	+0.36

Table 3. Continued.

Star	RA(2000)	DEC(2000)	V	$B-V$	$U-B$	Star	RA(2000)	DEC(2000)	V	$B-V$	$U-B$
161	23 59 26.17	+60 49 45.8	13.78	1.45	+1.09	239	00 00 04.71	+60 57 45.6	15.15	0.67	+0.44
162	23 59 41.19	+61 04 51.7	13.79	0.54	+0.27	240	23 59 19.79	+61 00 25.5	15.16	0.70	+0.13
163	00 01 38.40	+60 56 46.7	13.79	0.45	+0.29	241	23 59 39.28	+60 57 14.7	15.17	0.64	+0.31
164	00 01 13.36	+61 01 33.3	13.81	0.67	+0.05	242	00 00 22.59	+60 57 40.8	15.17	0.63	+0.09
165	23 59 20.85	+61 02 22.0	13.86	0.98	+0.61	243	23 59 53.74	+60 57 08.8	15.20	1.04	+0.39
166	00 00 05.82	+60 50 35.8	13.86	0.42	+0.00	244	00 00 04.46	+61 00 44.7	15.21	0.72	+0.28
167	00 00 02.37	+60 46 38.7	13.86	1.07	+0.04	245	00 00 06.29	+60 54 44.8	15.21	0.66	+0.29
168	23 59 04.31	+61 01 44.6	13.90	0.93	+0.84	246	00 00 38.77	+60 56 31.4	15.21	0.82	+0.49
169	00 00 00.15	+60 55 14.2	13.90	0.56	+0.06	247	23 59 50.61	+60 55 25.6	15.23	0.71	...
170	23 59 03.70	+61 01 50.1	13.91	0.88	+0.87	248	23 59 57.24	+60 55 02.8	15.24	0.69	+0.29
171	00 01 09.90	+60 52 54.7	13.93	0.94	+0.43	249	23 59 55.11	+60 53 44.8	15.26	0.71	+0.31
172	00 01 08.86	+60 58 34.1	13.94	1.04	+0.66	250	00 00 08.27	+60 56 42.6	15.35	0.94	+0.61
173	23 59 27.78	+60 55 30.8	13.97	0.67	+0.49	251	00 00 14.46	+60 57 47.6	15.42	0.77	+0.39
174	00 00 13.79	+61 01 04.7	13.98	0.98	+0.48	252	00 00 15.30	+60 54 57.0	15.42	0.72	...
175	00 00 26.02	+60 55 07.4	13.98	0.64	+0.20	253	00 00 31.15	+61 04 07.7	15.59	0.85	...
176	00 01 10.45	+60 58 30.7	13.99	0.68	+0.42	254	00 00 10.69	+60 55 58.4	15.62	0.79	...
177	00 00 11.44	+60 51 41.8	14.01	0.56	+0.12	255	00 00 06.19	+60 56 32.6	15.79	0.56	+0.23
178	00 01 16.45	+60 58 25.5	14.01	1.05	+0.21						

Table 4. CCD *UBV* Data for Stars in the Nucleus of Berkeley 58.

Star	RA(2000)	DEC(2000)	V	$B-V$	$U-B$	Star	RA(2000)	DEC(2000)	V	$B-V$	$U-B$
1001	23 59 13.34	+60 54 41.7	16.66	0.95	...	1192	23 59 59.79	+60 53 21.0	16.89	1.08	...
1002	23 59 13.58	+60 55 25.5	16.14	0.73	...	1193	00 00 00.31	+60 54 14.4	16.54	1.36	...
1003	23 59 12.82	+60 57 28.6	15.57	1.08	...	1194	00 00 04.01	+61 01 58.9	16.48	1.09	...
1004	23 59 12.99	+60 56 53.1	15.94	0.72	...	1195	00 00 01.08	+60 55 09.3	16.33	1.02	...
1005	23 59 12.00	+60 53 31.9	17.75	1.04	...	1196	00 00 02.86	+60 58 36.1	15.55	0.70	...
1006	23 59 14.92	+61 00 43.2	15.93	1.05	...	1197	00 00 04.28	+61 01 21.8	17.45	0.68	...
1007	23 59 15.93	+61 02 43.6	17.47	1.05	...	1199	00 00 04.99	+61 02 05.1	17.21	1.35	...
1008	23 59 16.20	+60 53 18.5	17.02	0.95	...	1200	00 00 03.25	+60 57 25.0	16.32	1.07	...
1009	23 59 15.49	+61 00 26.4	16.92	1.26	...	1201	00 00 01.48	+60 52 41.4	16.07	1.62	...
1010	23 59 16.63	+61 01 54.6	17.06	1.13	...	1203	00 00 01.53	+60 52 25.7	15.75	0.87	...
1011	23 59 14.72	+60 56 52.5	17.15	1.16	...	1205	00 00 05.80	+61 01 13.8	16.77	0.96	...
1012	23 59 14.95	+60 57 04.1	16.56	1.09	...	1206	00 00 02.37	+60 53 20.1	16.78	0.91	...
1013	23 59 16.05	+60 59 17.2	14.57	1.71	...	1207	00 00 02.97	+60 54 13.8	15.84	0.93	...
1014	23 59 13.40	+60 52 36.2	16.16	0.85	...	1208	00 00 02.45	+60 52 53.0	16.66	1.11	...
1015	23 59 14.93	+60 56 09.3	16.38	1.08	...	1209	00 00 04.49	+60 57 29.5	16.99	1.00	...
1016	23 59 13.64	+60 53 08.8	16.38	1.00	...	1211	00 00 05.98	+60 59 42.6	17.07	0.88	...
1017	23 59 15.15	+60 56 21.8	16.61	0.77	...	1213	00 00 04.22	+60 54 26.9	16.61	0.64	...
1018	23 59 15.09	+60 56 05.4	16.29	0.99	...	1214	00 00 04.64	+60 55 16.8	16.97	0.91	...
1019	23 59 15.91	+60 57 50.1	18.08	0.92	...	1215	00 00 03.56	+60 52 40.1	15.33	1.00	...
1020	23 59 17.35	+61 00 48.8	17.05	1.04	...	1216	00 00 08.29	+61 02 39.0	15.44	0.86	...
1021	23 59 16.51	+60 58 48.2	17.44	0.96	...	1218	00 00 05.99	+60 56 57.7	17.20	1.00	...
1022	23 59 16.58	+60 58 23.4	16.62	1.29	...	1220	00 00 07.02	+60 58 12.1	16.78	0.81	...
1023	23 59 17.72	+61 00 12.3	17.82	0.94	...	1222	00 00 05.08	+60 53 18.6	16.86	1.08	...
1024	23 59 15.99	+60 55 24.2	17.13	0.86	...	1223	00 00 05.00	+60 53 09.0	17.75	1.36	...
1025	23 59 17.49	+60 58 26.9	15.97	0.96	...	1224	00 00 07.16	+60 56 52.8	17.97	1.16	...
1026	23 59 17.43	+60 57 55.6	15.08	1.07	...	1225	00 00 05.25	+60 52 21.2	17.19	1.34	...
1027	23 59 16.20	+60 53 18.5	16.77	0.98	...	1227	00 00 06.82	+60 55 59.0	16.19	0.75	...
1028	23 59 17.45	+60 55 32.8	16.04	0.98	...	1228	00 00 08.19	+60 58 11.0	15.91	0.90	...
1029	23 59 19.01	+60 59 14.0	17.23	0.98	...	1229	00 00 06.17	+60 53 07.6	17.72	1.63	...
1030	23 59 17.76	+60 55 55.7	15.77	0.66	...	1230	00 00 06.64	+60 53 58.4	18.39	1.09	...
1031	23 59 17.95	+60 56 16.5	16.04	0.93	...	1231	00 00 08.71	+60 58 24.0	16.19	1.15	...
1034	23 59 20.75	+61 01 52.0	17.54	1.79	...	1232	00 00 07.31	+60 55 02.8	15.75	1.66	...
1035	23 59 20.78	+61 02 08.0	15.90	1.54	...	1233	00 00 09.48	+60 59 59.1	16.64	1.46	...
1036	23 59 19.06	+60 57 40.1	16.92	1.36	...	1234	00 00 09.94	+61 01 12.3	17.67	1.03	...
1037	23 59 21.76	+61 02 13.7	16.38	0.98	...	1235	00 00 10.21	+61 01 33.5	15.35	1.51	...
1038	23 59 21.29	+61 00 29.4	17.49	1.36	...	1236	00 00 07.39	+60 54 47.3	16.33	0.78	...
1039	23 59 20.03	+60 57 05.3	17.09	1.10	...	1238	00 00 11.06	+61 02 06.7	17.04	1.15	...
1040	23 59 19.65	+60 54 46.4	16.78	1.37	...	1240	00 00 08.12	+60 54 44.7	16.01	0.70	...

Table 4. CCD *UBV* Data for Stars in the Nucleus of Berkeley 58.

Star	RA(2000)	DEC(2000)	V	$B-V$	$U-B$	Star	RA(2000)	DEC(2000)	V	$B-V$	$U-B$
1041	23 59 18.71	+60 52 29.0	16.54	1.71	...	1242	00 00 07.23	+60 52 10.7	16.73	2.04	...
1042	23 59 21.26	+60 58 02.7	17.11	1.06	...	1243	00 00 08.18	+60 54 17.3	16.51	0.85	...
1043	23 59 19.98	+60 54 26.0	17.52	1.04	...	1244	00 00 12.27	+61 03 25.6	16.87	1.17	...
1044	23 59 21.95	+60 55 40.3	16.45	1.07	...	1246	00 00 11.22	+61 00 50.2	17.57	1.13	...
1047	23 59 21.29	+61 00 29.4	17.71	1.02	...	1248	00 00 09.33	+60 55 04.1	15.40	0.99	...
1048	23 59 25.23	+61 01 44.0	18.17	0.76	...	1249	00 00 07.98	+60 51 49.3	17.45	1.01	...
1050	23 59 25.80	+61 00 40.3	16.88	0.78	...	1251	00 00 11.50	+60 58 32.1	16.49	1.22	...
1051	23 59 25.17	+60 57 56.3	16.88	0.90	...	1254	00 00 10.42	+60 54 35.7	16.55	1.19	...
1052	23 59 23.33	+60 53 29.9	18.07	1.16	...	1255	00 00 13.91	+61 02 16.6	16.71	1.12	...
1053	23 59 24.72	+60 56 16.0	15.59	0.68	...	1256	00 00 12.77	+60 59 23.5	17.12	1.54	...
1054	23 59 25.52	+60 58 09.7	16.68	0.99	...	1258	00 00 13.64	+61 00 37.4	16.37	0.74	...
1056	23 59 28.15	+61 02 06.4	15.35	1.05	...	1260	00 00 15.23	+61 03 28.2	16.50	1.06	...
1057	23 59 28.38	+61 02 40.0	17.79	1.26	...	1261	00 00 11.36	+60 53 43.7	16.56	1.19	...
1058	23 59 25.80	+60 56 12.5	16.11	0.74	...	1262	00 00 15.48	+61 02 13.4	17.22	1.27	...
1059	23 59 27.56	+61 00 01.0	17.21	1.16	...	1263	00 00 13.05	+60 56 35.4	16.28	1.10	...
1060	23 59 28.13	+61 01 08.2	18.27	1.23	...	1267	00 00 13.09	+60 54 50.0	16.30	0.79	...
1061	23 59 27.05	+60 57 08.2	16.71	1.09	...	1268	00 00 13.36	+60 55 30.2	16.32	0.81	...
1062	23 59 27.87	+60 58 36.6	16.25	0.79	...	1270	00 00 14.81	+60 58 25.1	15.14	0.83	+0.39
1063	23 59 27.43	+60 56 19.0	16.13	0.81	...	1271	00 00 12.88	+60 53 46.9	16.18	0.99	...
1064	23 59 28.87	+60 59 01.0	17.09	1.58	...	1272	00 00 14.21	+60 56 52.2	16.68	0.84	...
1066	23 59 31.06	+61 03 11.5	17.93	0.73	...	1273	00 00 16.48	+61 01 21.1	16.21	1.21	...
1067	23 59 29.96	+61 00 22.6	16.55	0.79	...	1276	00 00 15.16	+60 56 22.6	16.45	0.90	...
1068	23 59 32.09	+61 03 09.1	15.75	0.71	...	1277	00 00 18.04	+61 02 55.1	15.96	1.18	...
1069	23 59 28.50	+60 53 37.0	16.50	1.90	...	1278	00 00 15.74	+60 57 35.8	15.97	0.73	...
1070	23 59 30.44	+60 57 43.2	16.01	0.80	...	1280	00 00 15.73	+60 56 08.6	14.63	0.62	...
1071	23 59 28.90	+60 53 12.9	15.76	0.77	...	1281	00 00 19.00	+61 03 27.4	16.65	1.19	...
1072	23 59 33.99	+61 03 29.5	16.00	1.24	...	1282	00 00 16.52	+60 57 18.9	15.61	0.66	...
1073	23 59 34.17	+61 03 37.8	16.26	1.10	...	1284	00 00 17.90	+61 00 03.0	17.22	1.01	...
1074	23 59 29.68	+60 52 38.3	15.41	0.84	...	1285	00 00 16.72	+60 56 21.5	16.29	0.79	...
1075	23 59 30.93	+60 54 47.6	14.80	0.79	...	1286	00 00 16.19	+60 54 46.9	16.00	0.80	...
1076	23 59 32.61	+60 57 52.0	17.72	1.53	...	1288	00 00 18.80	+61 00 28.6	16.45	1.10	...
1077	23 59 33.73	+60 59 41.7	16.10	1.17	...	1289	00 00 15.18	+60 52 03.5	15.89	0.69	...
1078	23 59 34.68	+61 01 48.7	15.65	0.98	...	1291	00 00 17.51	+60 54 33.5	16.94	0.93	...
1079	23 59 31.86	+60 54 42.7	17.01	1.04	...	1292	00 00 19.32	+60 58 39.6	17.47	1.00	...
1080	23 59 31.86	+60 54 42.7	16.97	1.49	...	1296	00 00 17.29	+60 53 12.4	15.17	0.63	+0.35
1081	23 59 32.85	+60 56 59.5	16.14	1.15	...	1297	00 00 18.05	+60 54 52.8	18.48	0.75	...
1082	23 59 34.12	+60 59 35.0	17.33	1.21	...	1300	00 00 17.98	+60 53 30.9	16.95	0.94	...
1083	23 59 34.86	+61 00 37.8	18.19	1.32	...	1301	00 00 19.95	+60 57 43.7	16.49	0.83	...
1084	23 59 35.83	+61 02 46.5	17.06	1.23	...	1302	00 00 22.49	+61 03 13.7	17.65	1.30	...
1085	23 59 33.94	+60 58 15.1	15.44	1.02	...	1303	00 00 19.95	+60 56 56.2	16.21	0.76	...
1086	23 59 32.21	+60 54 02.5	17.03	1.15	...	1304	00 00 19.64	+60 55 42.7	15.41	0.82	+0.40
1087	23 59 37.51	+61 03 44.1	17.09	1.08	...	1305	00 00 19.28	+60 54 20.6	17.33	0.88	...
1089	23 59 36.54	+61 00 02.4	16.53	0.98	...	1306	00 00 22.71	+61 01 56.3	15.56	0.97	...
1090	23 59 36.12	+60 58 55.6	17.09	0.96	...	1308	00 00 20.21	+60 55 46.7	16.06	0.82	...
1091	23 59 34.93	+60 55 57.4	16.78	0.86	...	1309	00 00 22.89	+61 01 31.3	15.37	0.69	...
1092	23 59 37.51	+61 01 02.7	17.19	1.11	...	1310	00 00 19.89	+60 54 14.5	17.37	0.94	...
1093	23 59 34.11	+60 52 36.4	17.45	1.28	...	1312	00 00 23.20	+61 00 33.3	16.07	0.97	...
1094	23 59 35.83	+60 56 22.0	15.86	0.73	...	1313	00 00 19.55	+60 52 05.6	17.12	1.32	...
1095	23 59 36.21	+60 56 32.0	17.57	1.22	...	1316	00 00 22.99	+60 58 18.8	16.89	0.91	...
1096	23 59 37.50	+60 59 19.8	16.08	1.68	...	1317	00 00 22.86	+60 57 46.9	16.83	1.07	...
1097	23 59 35.15	+60 52 52.6	15.92	1.19	...	1318	00 00 22.56	+60 56 45.6	15.96	0.95	...
1098	23 59 36.03	+60 54 59.3	16.84	1.25	...	1319	00 00 22.88	+60 57 13.2	18.10	0.97	...
1099	23 59 39.28	+61 02 43.6	16.79	0.52	...	1321	00 00 25.60	+61 02 35.0	17.07	0.99	...
1100	23 59 39.64	+61 02 33.1	17.46	0.83	...	1322	00 00 23.71	+60 57 48.7	15.95	1.13	...
1101	23 59 37.38	+60 55 12.4	17.15	1.26	...	1325	00 00 22.62	+60 53 54.3	16.47	0.84	...
1102	23 59 38.35	+60 55 38.7	16.63	0.75	...	1327	00 00 23.38	+60 55 03.2	16.46	0.85	...
1103	23 59 40.10	+60 59 35.4	15.86	1.60	...	1329	00 00 24.44	+60 55 48.5	17.27	1.82	...
1104	23 59 38.95	+60 56 32.1	17.02	1.16	...	1330	00 00 25.71	+60 58 11.2	16.87	0.95	...
1106	23 59 41.29	+61 00 12.6	15.25	0.96	...	1331	00 00 27.70	+61 02 34.9	16.66	1.06	...
1108	23 59 38.51	+60 52 55.3	16.57	0.77	...	1334	00 00 25.39	+60 56 42.7	16.73	1.13	...
1110	23 59 40.09	+60 55 57.7	17.86	1.22	...	1335	00 00 26.62	+60 58 55.3	16.69	1.00	...
1112	23 59 43.52	+61 03 38.3	16.36	1.10	...	1336	00 00 28.63	+61 02 50.2	17.01	1.02	...

Table 4. Continued.

Star	RA(2000)	DEC(2000)	V	$B-V$	$U-B$	Star	RA(2000)	DEC(2000)	V	$B-V$	$U-B$
1113	23 59 43.33	+61 02 52.0	16.41	0.89	...	1337	00 00 25.72	+60 56 07.5	16.60	0.85	...
1114	23 59 39.50	+60 53 42.6	16.37	0.97	...	1338	00 00 24.86	+60 54 02.0	16.25	1.18	...
1115	23 59 40.32	+60 55 03.8	15.39	0.79	+0.25	1340	00 00 27.13	+60 58 13.9	18.06	1.69	...
1116	23 59 40.65	+60 54 36.6	16.49	0.82	...	1341	00 00 26.64	+60 56 47.9	16.46	1.01	...
1117	23 59 41.73	+60 56 35.4	15.32	0.86	...	1343	00 00 26.18	+60 54 16.6	16.25	1.04	...
1119	23 59 43.50	+60 58 13.5	17.14	1.22	...	1344	00 00 29.86	+61 01 29.8	16.83	1.34	...
1120	23 59 45.69	+61 02 26.1	15.32	1.07	...	1345	00 00 25.91	+60 52 38.3	17.19	0.86	...
1121	23 59 42.53	+60 53 55.6	16.28	0.72	...	1346	00 00 29.97	+61 01 08.2	17.60	0.84	...
1122	23 59 46.20	+61 02 01.7	17.52	1.25	...	1347	00 00 27.25	+60 54 15.9	16.34	0.97	...
1123	23 59 43.41	+60 55 23.6	17.04	0.84	...	1348	00 00 28.62	+60 56 47.1	16.96	1.08	...
1125	23 59 44.33	+60 56 58.6	16.72	0.89	...	1349	00 00 28.30	+60 55 49.0	15.64	0.72	...
1126	23 59 43.56	+60 55 04.0	16.21	2.03	...	1350	00 00 27.82	+60 53 48.3	16.70	1.70	...
1127	23 59 47.02	+61 03 03.1	17.31	0.91	...	1351	00 00 27.71	+60 53 14.2	15.58	0.80	+0.36
1128	23 59 46.62	+61 01 32.7	15.44	0.84	...	1352	00 00 31.85	+61 02 28.5	17.52	1.11	...
1129	23 59 46.50	+60 59 05.0	16.56	1.29	...	1353	00 00 31.05	+61 00 30.3	16.71	0.95	...
1131	23 59 45.21	+60 55 29.1	16.97	0.88	...	1354	00 00 32.37	+61 03 24.7	17.55	1.31	...
1132	23 59 48.63	+61 02 17.7	16.29	1.05	...	1355	00 00 28.37	+60 53 26.7	18.03	1.30	...
1133	23 59 45.25	+60 53 56.4	17.55	1.09	...	1356	00 00 31.96	+61 00 51.7	16.23	0.84	...
1134	23 59 45.19	+60 53 10.1	16.73	1.04	...	1357	00 00 29.40	+60 54 53.3	17.67	1.61	...
1135	23 59 46.91	+60 57 15.7	16.02	0.86	...	1358	00 00 33.10	+61 02 31.4	15.83	1.57	...
1136	23 59 49.94	+61 02 53.1	17.51	1.62	...	1360	00 00 31.91	+60 55 55.0	16.47	1.13	...
1137	23 59 46.12	+60 53 22.2	16.08	0.95	...	1361	00 00 35.02	+61 02 12.6	17.79	0.75	...
1138	23 59 49.74	+61 00 38.8	15.68	0.70	...	1362	00 00 34.55	+61 00 38.4	17.98	1.19	...
1140	23 59 50.67	+61 01 41.2	15.58	1.08	...	1366	00 00 31.86	+60 51 48.7	15.76	0.89	...
1141	23 59 48.83	+60 56 27.6	15.59	0.43	...	1368	00 00 35.45	+60 59 16.8	17.76	1.30	...
1142	23 59 48.58	+60 54 55.9	16.75	0.75	...	1369	00 00 34.42	+60 56 17.0	16.72	1.68	...
1143	23 59 48.15	+60 52 45.3	17.97	1.15	...	1370	00 00 34.37	+60 55 24.0	16.60	1.62	...
1145	23 59 52.16	+61 01 56.9	15.26	0.67	...	1371	00 00 34.24	+60 53 47.0	16.69	1.01	...
1146	23 59 49.31	+60 54 51.9	16.66	1.48	...	1372	00 00 34.82	+60 54 43.0	16.20	0.71	...
1147	23 59 49.43	+60 54 30.0	17.56	1.22	...	1373	00 00 34.78	+60 53 52.4	15.45	1.00	...
1148	23 59 51.90	+60 59 21.9	16.51	1.08	...	1374	00 00 36.03	+60 54 42.1	17.24	1.15	...
1149	23 59 51.37	+60 58 06.1	15.19	0.82	...	1375	00 00 39.55	+61 02 38.1	16.98	1.15	...
1152	23 59 53.67	+61 02 36.0	17.47	1.18	...	1376	00 00 37.12	+60 57 02.4	16.00	1.08	...
1153	23 59 54.32	+61 03 11.1	16.90	0.82	...	1377	00 00 39.04	+61 00 55.9	16.67	1.34	...
1154	23 59 51.16	+60 55 14.9	17.80	1.65	...	1379	00 00 37.67	+60 57 59.9	15.55	1.02	...
1155	23 59 52.79	+60 58 19.0	17.38	0.83	...	1381	00 00 40.36	+61 02 47.1	15.80	1.67	...
1157	23 59 53.48	+60 59 19.6	15.41	0.78	...	1382	00 00 40.89	+61 03 10.5	15.40	1.48	...
1158	23 59 53.70	+60 58 05.2	15.70	1.13	...	1383	00 00 37.34	+60 55 18.2	17.14	0.99	...
1159	23 59 53.37	+60 56 31.1	16.86	0.86	...	1384	00 00 38.06	+60 56 22.3	17.04	1.35	...
1161	23 59 53.61	+60 56 42.3	16.31	0.64	...	1385	00 00 39.47	+60 59 25.0	17.78	1.05	...
1162	23 59 53.84	+60 56 47.8	17.30	1.07	...	1386	00 00 36.10	+60 51 55.4	17.95	0.91	...
1163	23 59 55.67	+61 01 05.6	16.52	2.00	...	1387	00 00 41.30	+61 02 53.3	15.70	1.15	...
1164	23 59 59.66	+60 58 23.2	15.94	0.88	...	1388	00 00 36.89	+60 52 34.9	16.71	0.75	...
1165	23 59 55.58	+60 58 07.6	15.57	0.97	...	1390	00 00 39.24	+60 56 41.0	16.81	1.00	...
1166	23 59 55.72	+60 58 02.6	16.54	1.06	...	1391	00 00 39.73	+60 56 18.0	17.05	0.98	...
1167	23 59 56.69	+61 00 12.9	17.40	1.22	...	1392	00 00 40.08	+60 56 38.0	15.57	1.16	...
1170	23 59 55.08	+60 52 26.3	16.83	1.07	...	1393	00 00 39.00	+60 54 19.5	16.79	0.84	...
1171	23 59 56.83	+60 55 47.9	16.50	0.80	...	1395	00 00 39.72	+60 54 38.8	16.34	1.74	...
1172	23 59 59.55	+61 01 53.2	16.69	0.94	...	1396	00 00 43.80	+61 02 59.9	15.14	1.08	...
1173	23 59 57.85	+60 57 25.1	16.45	0.98	...	1397	00 00 41.17	+60 54 50.4	15.25	1.12	...
1174	00 00 00.65	+61 03 36.3	15.55	1.06	...	1398	00 00 40.57	+60 52 41.2	17.19	0.86	...
1176	23 59 56.51	+60 52 55.0	16.74	1.11	...	1399	00 00 38.87	+60 53 10.0	16.01	0.68	...
1177	00 00 00.62	+61 01 12.0	17.52	1.34	...	1400	00 00 43.57	+60 58 21.3	15.45	0.76	...
1178	00 00 00.20	+60 59 46.3	17.25	0.81	...	1401	00 00 44.40	+60 59 36.9	18.65	1.07	...
1179	00 00 01.88	+61 03 03.4	15.38	1.07	...	1402	00 00 43.42	+60 56 29.0	15.88	0.82	...
1182	00 00 00.15	+60 57 08.5	15.28	1.01	...	1403	00 00 42.83	+60 54 31.8	15.47	0.79	...
1183	00 00 00.26	+60 56 27.9	16.88	1.92	...	1404	00 00 43.86	+60 54 44.7	16.30	0.96	...
1184	23 59 58.63	+60 52 34.4	16.41	1.09	...	1405	00 00 43.28	+60 52 49.2	17.41	0.98	...
1185	00 00 00.30	+60 56 02.3	16.11	0.75	...	1406	00 00 44.94	+60 55 57.8	16.27	1.06	...
1188	23 59 58.82	+60 52 06.4	15.79	0.73	...	1407	00 00 44.69	+60 55 09.5	16.07	1.10	...
1189	23 59 59.50	+60 53 34.1	17.02	1.53	...	1409	00 00 44.26	+60 52 52.3	15.79	0.76	...
1190	00 00 03.53	+61 02 52.6	16.24	1.22	...	1410	00 00 44.22	+60 52 20.0	16.66	1.32	...
1191	00 00 00.29	+60 54 38.8	15.95	0.94	...	1411	00 00 49.52	+61 02 30.2	15.75	1.66	...